AGU PUBLICATIONS

Geophysical Research Letters

RESEARCH LETTER
10.1002/2017GL074405

Key Points:
- Observations show a robust O_3-CO regression in the boundary layer in daytime over the eastern U.S. in summer
- Oxidation of biogenic isoprene makes a significant contribution to the observed boundary layer O_3-CO regression slope
- The consistent enhancement of O_3 relative to CO in the boundary layer provides a useful constraint on model photochemistry and emissions

Supporting Information:
- Supporting Information S1

Correspondence to:
Y. Wang,
yuhang.wang@eas.gatech.edu

Citation:
Cheng, Y., Y. Wang, Y. Zhang, G. Chen, J. H. Crawford, M. M. Kleb, G. S. Diskin, and A. J. Weinheimer (2017), Large biogenic contribution to boundary layer O_3-CO regression slope in summer, *Geophys. Res. Lett.*, *44*, doi:10.1002/2017GL074405.

Received 4 JUN 2017
Accepted 17 JUN 2017
Accepted article online 20 JUN 2017

Large biogenic contribution to boundary layer O_3-CO regression slope in summer

Ye Cheng[1], Yuhang Wang[1], Yuzhong Zhang[1], Gao Chen[2], James H. Crawford[2], Mary M. Kleb[2], Glenn S. Diskin[2], and Andrew J. Weinheimer[3]

[1]School of Earth and Atmospheric Sciences, Georgia Institute of Technology, Atlanta, Georgia, USA, [2]NASA Langley Research Center, Hampton, Virginia, USA, [3]Atmospheric Chemistry Observations and Modeling Laboratory, National Center for Atmospheric Research, Boulder, Colorado, USA

Abstract Strong correlation between O_3 and CO was observed during the Deriving Information on Surface Conditions from Column and Vertically Resolved Observations Relevant to Air Quality (DISCOVER-AQ) aircraft experiment in July 2011 over the Washington-Baltimore area. The observed correlation does not vary significantly with time or altitude in the boundary layer. The observations are simulated well by a regional chemical transport model. We analyze the model results to understand the factors contributing to the observed O_3-CO regression slope, which has been used in past studies to estimate the anthropogenic O_3 production amount. We trace separately four different CO sources: primary anthropogenic emissions, oxidation of anthropogenic volatile organic compounds, oxidation of biogenic isoprene, and transport from the lateral and upper model boundaries. Modeling analysis suggests that the contribution from biogenic isoprene oxidation to the observed O_3-CO regression slope is as large as that from primary anthropogenic CO emissions. As a result of decrease of anthropogenic primary CO emissions during the past decades, biogenic CO from oxidation of isoprene is increasingly important. Consequently, observed and simulated O_3-CO regression slopes can no longer be used directly with an anthropogenic CO emission inventory to quantify anthropogenic O_3 production over the United States. The consistent enhancement of O_3 relative to CO observed in the boundary layer, as indicated by the O_3-CO regression slope, provides a useful constraint on model photochemistry and emissions.

1. Introduction

Tropospheric ozone (O_3) and carbon monoxide (CO) are major pollutants in the troposphere [e.g., *Logan et al.*, 1981; *Wang and Jacob*, 1998; *Wang et al.*, 1998; *Lelieveld and Dentener*, 2000]. A linear relationship between the two pollutants is often observed and simulated in the lower atmosphere [e.g., *Parrish et al.*, 1993; *Chin et al.*, 1994; *Buhr et al.*, 1996; *Parrish et al.*, 1998; *Cardenas et al.*, 1998; *Li et al.*, 2002; *Cooper et al.*, 2002a, 2002b; *Honrath et al.*, 2004; *Mao and Talbot*, 2004; *Huntrieser et al.*, 2005]. The observed slope of O_3 to CO at ~0.3 has been used to estimate net anthropogenic O_3 production [e.g., *Parrish et al.*, 1993; *Chin et al.*, 1994]. However, these and subsequent studies also noted the uncertainty in using the O_3-CO slope approach. For example, O_3 deposition will lead to slopes <0.3 in the region of anthropogenic emission area [*Chin et al.*, 1994; *Parrish et al.*, 1998; *Cardenas et al.*, 1998; *Li et al.*, 2002; *Mao and Talbot*, 2004; *Real et al.*, 2008] and stratospheric intrusion will affect the slopes at high-altitude regions [*Parrish et al.*, 1998].

Another factor that may lead to biases using this approach is the contribution of biogenic emissions to CO production. *Chin et al.* [1994] suggested that biogenic isoprene oxidation might be a very important process. In regions of large biogenic emissions, oxidation of isoprene far exceeds oxidation of anthropogenic volatile organic compounds (VOCs), leading to production of both O_3 and CO [*Guenther et al.*, 1995; *Atkinson and Arey*, 1998; *Pierce et al.*, 1998; *Hudman et al.*, 2008; *Pang et al.*, 2009; *Choi et al.*, 2010; *Geng et al.*, 2011; *Lee et al.*, 2014; *Zhang and Wang*, 2016]. As anthropogenic emissions decrease in the U.S. [e.g., *Parrish et al.*, 2002; *Hassler et al.*, 2016], the relative importance of biogenic emissions increases. However, the effects of biogenic emissions on the correlation between O_3 and CO and its implications for using the slope approach to estimate anthropogenic O_3 production rate have not been studied in detail.

Extensive sampling of O_3, CO, and other trace gases was conducted during the NASA Earth Venture airborne campaign, Deriving Information on Surface Conditions from Column and Vertically Resolved Observations

Relevant to Air Quality (DISCOVER-AQ), in July 2011 around the Baltimore-Washington area (see the online data archive: http://www-air.larc.nasa.gov/missions/discover-aq/discover-aq.html for detailed description of the research flights). In this study, we apply a 3-D chemical transport model to quantitatively study factors contributing to the observed O_3-CO correlation and regression slope and examine the implications for using the observed correlation. We describe the model, observational data set, and analysis method in section 1. Simulation results and interpretation of the O_3-CO regression slope are described in section 3. Conclusions and implications are given in section 4.

2. Methods

The 3-D Regional chEmical trAnsport Model (REAM) has been applied in a number of tropospheric chemistry and transport studies over North America and East Asia [e.g., *Choi et al*., 2005, 2008a, 2008b; *Jing et al*., 2006; *Liu et al*., 2010, 2012a, 2012b, 2014; *Wang et al*., 2006, 2007; *Yang et al*., 2011; *Zeng et al*., 2003, 2006; *Zhao and Wang*, 2009; *Zhao et al*., 2009a, 2009b, 2010; *Gu et al*., 2013, 2014, 2016; *Zhang et al*., 2016; *Zhang and Wang*, 2016; *Zhang et al*., 2017]. The model has a horizontal resolution of 36×36 km^2. Transport is driven by the Weather Research and Forecasting (WRF) model-assimilated meteorological fields constrained by the Climate Forecast System Reanalysis products (http://cfs.ncep.noaa.gov/cfsr). The WRF model domain is 10 grid cell larger than that of REAM on each lateral side. The chemistry mechanism in REAM is adopted from the GEOS-Chem model (v9-02) [*Bey et al*., 2001] with updates of kinetics data (http://jpldataeval.jpl.nasa.gov). The anthropogenic emission inventory used in the model is the 2011 National Emission Inventory (https://www.epa.gov/air-emissions-inventories/2011-national-emissions-inventory-nei-data). The biogenic isoprene emissions are computed using the Model of Emissions of Gases and Aerosols from Nature version 2.1 [*Guenther et al*., 2012]. Initial and boundary conditions for chemical tracers are taken from the GEOS-Chem (v9-02) $2° \times 2.5°$ simulation results [*Bey et al*., 2001].

The observational data were obtained during the NASA 2011 DISCOVER-AQ airborne campaign, sampling from Washington's Beltway northeast to Baltimore and continuing on to the Delaware State line and occasionally over the Chesapeake Bay. The vertical structures of pollutants were measured through 253 daytime vertical profiles from 300 m to 5 km over six selected locations during 14 flights by NASA's P-3B aircraft between June 27 and July 31. CO was measured by a diode laser spectrometer [*Sachse et al*., 1987] with a 2% uncertainty. NO, NO_2, and O_3 were measured by the National Center for Atmospheric Research four-channel chemiluminescence instrument [*Brent et al*., 2015] with 10%, 15%, and 5% uncertainties, respectively. CH_2O was measured by a difference frequency generation absorption spectrometer [*Weibring et al*., 2010] with a 4% uncertainty. Isoprene was measured by a proton-transfer-reaction mass spectrometer [*Lindinger et al*., 1998] with a 10% uncertainty.

The model domain of REAM and locations of DISCOVER-AQ observations are shown in Figure S1 in the supporting information. There are 253 aircraft spirals around 6 locations [*Zhang et al*., 2016]. To evaluate model simulations with the observations, we first identify the model grid cells corresponding to the locations of aircraft spirals. These model profiles are then archived at the time of aircraft sampling. The corresponding aircraft and model data are used in correlation analysis, and the averaged model vertical profiles are also compared to the observations.

In order to analyze the attributions of the observed O_3-CO relationship, we trace separately four different CO sources: primary anthropogenic emissions ($CO_{anthroCO}$), the oxidation of anthropogenic VOCs ($CO_{anthroVOCs}$), the oxidation of biogenic isoprene ($CO_{bioISOP}$), and transport from model lateral and upper boundaries (CO_{BC}). We do not account for other biogenic VOCs since isoprene is much more abundant than the other species providing the source for the vast majority biogenic CO [e.g., *Kesselmeier and Staudt*, 1999; *Lathière et al*., 2006; *Guenther et al*., 2012; *Sindelarova et al*., 2014]. In tagged-tracer simulations, relevant species and radicals, such as O_3, NO_x, and HO_x (OH and HO_2), are fixed using results archived from the standard simulation. The sum of the four individual tracers is within 5% of the simulated total CO concentrations in the standard simulation for grid cells over the Washington-Baltimore region. Minor scaling adjustments, assuming that relative CO attributions stay the same, are added in postprocessing to ensure that the sum of the CO tracers is the same as the total CO for each grid cell in the standard simulation. With

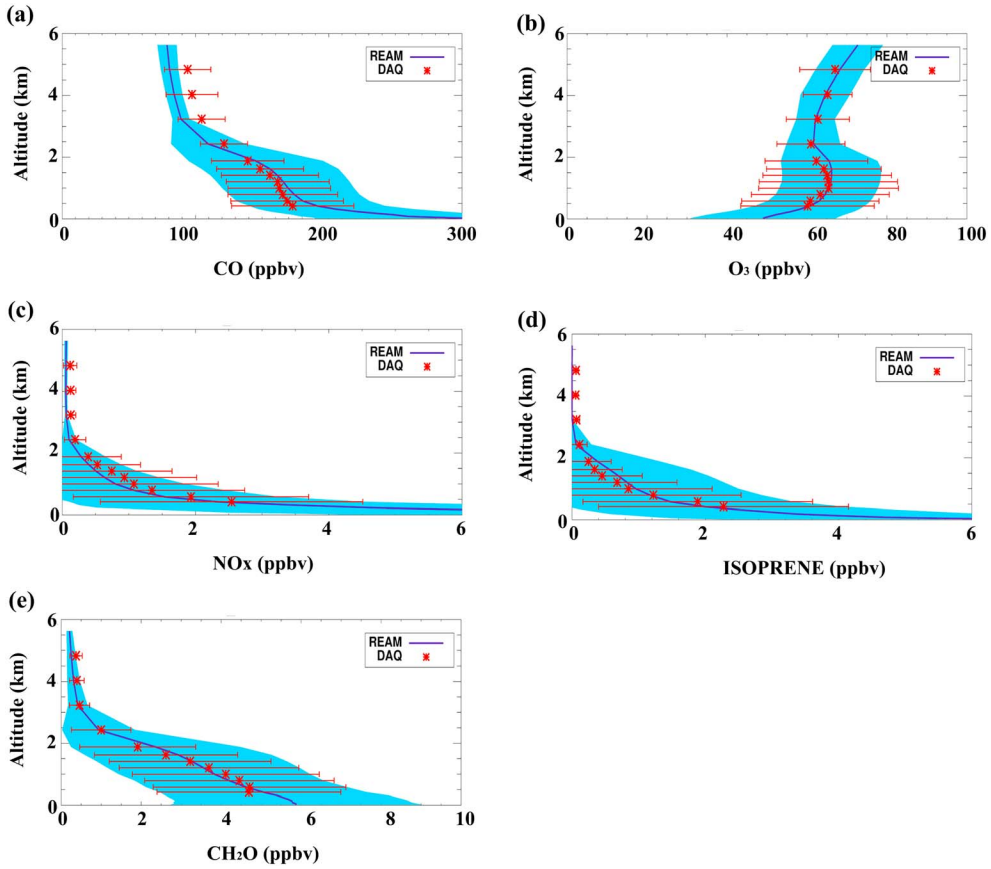

Figure 1. Observed and simulated vertical profiles of (a) CO, (b) O_3, (c) NO_x, (d) isoprene, and (e) CH_2O in July 2011 during the DISCOVER-AQ experiment. DAQ represents the DISCOVER-AQ data. The red horizontal bars show the observed standard deviations; the shaded blue areas denote the simulated standard deviations. For comparison purposes, the observational data are binned vertically according to the vertical grid structure in the model.

simulated CO attribution results, we can decompose the O_3-CO regression slope into four subslopes of the corresponding CO tracers (equation (1); see the Appendix)

$$\text{Least}-\text{squares regression slope} = \frac{Cov(CO_{anthroCO}, O_3)}{Var(CO_{total})} + \frac{Cov(CO_{anthroVOCs}, O_3)}{Var(CO_{total})} + \frac{Cov(CO_{BC}, O_3)}{Var(CO_{total})} + \frac{Cov(CO_{biolSOP}, O_3)}{Var(CO_{total})} \quad (1)$$

where *Cov* and *Var* denote the covariance and variance, respectively. Equation (1) shows that the contributions of each CO tracer to the O_3-CO regression slope are proportional to its covariance with O_3. It is therefore possible to have both positive and negative slope contributions.

3. Results

We first evaluate simulated vertical profiles of O_3, CO, NO_x, isoprene, and CH_2O with DISCOVER-AQ observations (Figure 1). CH_2O is an intermediate product of anthropogenic and biogenic VOC oxidation; NO_x is mainly from anthropogenic emissions and isoprene is biogenic, both of which contribute to O_3 production [e.g., *Zhang et al.*, 2016]. The model reproduces well the observed vertical profiles of these species.

The short-lived NO_x, isoprene, and CH_2O decrease rapidly from the surface to the free troposphere, reflecting in part the dominant NO_x and VOCs sources near the surface and rapid photochemical loss in the atmosphere. The nearly linear decrease of CH_2O, in contrast to the exponential decreases of NO_x and isoprene,

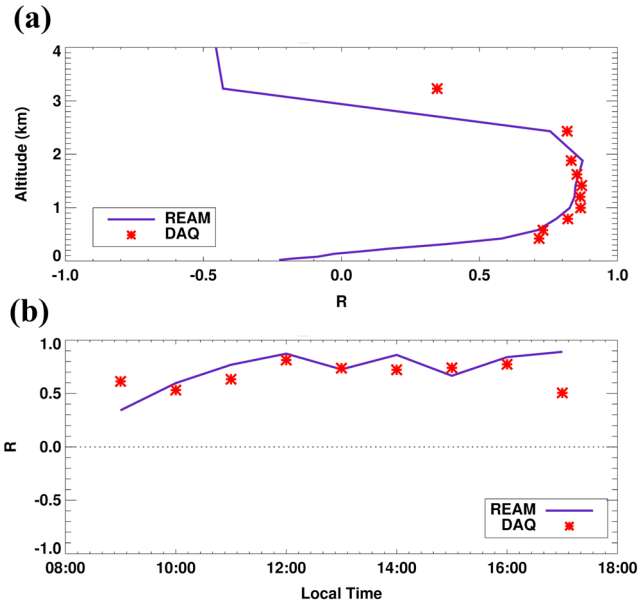

Figure 2. Observed and simulated O_3-CO correlation coefficients (R) as a function of (a) altitude for daytime of 10 A.M. to 4 P.M. and (b) local time for altitude of 0.3–2.5 km. The R values are computed using the observation or corresponding model data (for the entire DISCOVER-AQ experiment) at a given altitude bin or a given time period.

reflects that its atmospheric secondary (photochemical) source is much larger than primary emissions. Ozone has a peak in the middle of the boundary layer due in part to dry deposition loss of ozone and in part to decreasing photochemical production and loss with altitude. It increases with altitude in the free troposphere reflecting the increase of chemical lifetime with altitude.

Using results from tagged-tracer simulation, we can attribute the vertical profile of CO to four different sources (Figure S2). The boundary contribution does not vary significantly with altitude. The contribution by primary emissions from the surface decreases with altitude. The contributions by secondary productions from biogenic or anthropogenic VOCs do not have as large a decrease as those of primary emissions since secondary production takes place mostly from late morning to the afternoon when the boundary layer is well mixed, while the shallow boundary layer in early morning (as early as 5 A.M.) can lead to a large gradient of surface emitted species such as CO [e.g., *Zhang et al*., 2016]. The rapid decrease of secondary CO from the boundary layer to the free troposphere reflects slow vertical transport between the two layers. Clearly, secondary CO is a major factor shaping its observed vertical variation.

The daytime hourly variations of the selected species averaged from 300 m to 2.5 km are shown in Figure S3. In general, the variation is much less than in the vertical. The temporal change of NO_x is insignificant while O_3, CO, isoprene, and CH_2O tend to accumulate in the lower atmosphere from morning to afternoon. The observed variations are well simulated by the model, providing further evidence for the good model performance during the measurement period.

Correlations between chemical species can be used effectively to diagnose atmospheric processes [e.g., *Parrish et al*., 1993; *Chin et al*., 1994; *Wang and Zeng*, 2004; *Koo et al*., 2012]. We compare simulated O_3-CO correlations to the observations as a function of altitude or time of the day in Figure 2. The observations show a narrow range of R value (~0.75) from 1 km to the top of the boundary layer (~2.5 km). Below 1 km, the observations indicate a trend of decreasing R value with altitude down to 300 m. The model results are similar to the observed values and also show lower correlations near the surface and in the free troposphere. In the free troposphere, CO is dominated by the contribution by boundary layer transport (Figure S2), which is not related to O_3 production in the boundary layer. Near the surface, CO is dominated by surface primary emissions, which are not directly related to O_3 production either. Furthermore, mixing of fresh emissions with photochemically aged air in the boundary layer leads to an increase of O_3 but a decrease of CO since the large vertical gradients of O_3 and CO near the surface have opposite signs (Figure 1). In the middle and upper boundary layer, the relative contribution by photochemical CO production increases. Therefore, the concurrent photochemical production of O_3 and CO is likely the major factor contributing to the observed positive correlation between O_3 and CO. We quantify this contribution by decomposing the O_3-CO regression slope into the different CO sources.

Figure 2 also shows the observed O_3-CO correlation coefficient as a function of time of the day with data from 300 m to 2.5 km. This R value represents the spatial correlation in a given hour. It is somewhat lower than the temporal correlation discussed previously. The value ranges from 0.5 to 0.6 in the morning and 0.6 to 0.8 in

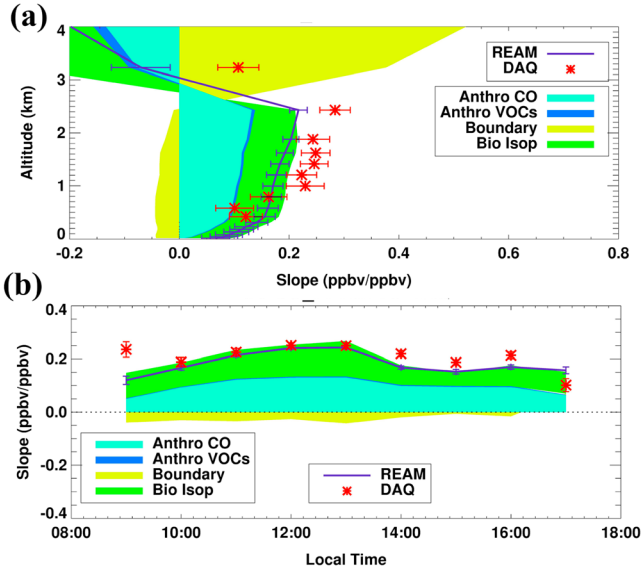

Figure 3. Same as in Figure 2 but for the observed and simulated vertical profiles and diurnal variations of the CO-O_3 regression slope and subslopes. The components of subslopes, due to varied CO sources, are shown using areas filled with different colors. The legends for different CO sources are the same as in equation (1). The (a) horizontal bars and (b) vertical bars show the observed or simulated standard deviation of the regression slope. The slope and subslope values are computed using the observations or model data at a given altitude bin or for a given time period.

most of the afternoon. The model is in good agreement with the observations except the overestimation at 5 P.M.

Figure 3 compares the observed and simulated O_3-CO regression slope. The O_3-CO regression slope at a given altitude is underestimated by the model at 1–2.5 km by ~20% but is overestimated below 1 km. At 3 km, the model shows a negative regression slope value opposite to the observations. However, the observed decrease of the regression slope below 1 km and above 2.5 km is captured by the model. The observed O_3-CO regression slope at a given hour is better simulated than that at a given altitude. The O_3-CO regression slope of 0.1–0.3 during the DISCOVER-AQ experiment is consistent with the previous reports for land areas [e.g., *Chin et al.*, 1994]. We apply the model results to understand the relative contributions of CO sources to the O_3-CO regression slope (equation (1)).

In the lower atmosphere (below 2.5 km), where the model results are in reasonably good agreement with the observations, Figure 3 shows that the contribution of CO from biogenic isoprene oxidation is nearly as large as that of primary anthropogenic CO. In particular, the relative importance of biogenic CO increases toward the surface. These two contributions account for $>$90% of the O_3-CO regression slope in the lower atmosphere ($<$2.5 km). The contributions of CO from photochemical oxidation of anthropogenic VOCs and from the model boundaries are minor in comparison. In the free troposphere (above 2.5 km), Figure 3 shows that the contributions by anthropogenic CO and VOCs and biogenic isoprene to the O_3-CO regression slope are negative. This is because air near the top boundary layer is enriched in these CO tracers but not in O_3 relative to low free tropospheric air (Figure 1). The positive contribution by CO transported from the (lateral) boundary reflects largely a general south-to-north positive gradient in free tropospheric CO and O_3 in the model.

Our analysis of the DISCOVER-AQ measurements suggests that the previously used hypothesis, i.e., the regression slope of O_3 to CO was controlled by anthropogenic emissions and the photochemical oxidation of anthropogenic ozone precursors [e.g., *Parrish et al.*, 1993; *Chin et al.*, 1994], is no longer valid. However, a caveat is that anthropogenic emissions of CO decreased by ~46% from 1993 to 2011 (https://www.epa.gov/air-emissions-inventories/air-pollutant-emissions-trends-data). The large decrease of anthropogenic CO emissions can lead to the invalidity of the hypothesis. We carry out a sensitivity simulation in which the anthropogenic primary CO emissions are doubled (Figure S4). After doubling anthropogenic primary CO emissions, anthropogenic CO accounts for a larger fraction in the lower troposphere. More drastic change is found in the O_3-CO regression slope, ~75% of which in the lower troposphere are due to anthropogenic emissions, making the previous hypothesis a good approximation. As anthropogenic emissions continue decreasing, we expect that the biogenic contribution to the O_3-CO regression slope will increase in the future.

4. Conclusions and Implications

The extensive measurements in the lower atmosphere during the DISCOVER-AQ experiment over the Washington-Baltimore area in July 2011 are analyzed in this study to understand the contributions to the

O_3-CO regression slope from different CO sources using REAM model. The observed vertical and temporal variations of O_3, CO, NO_x, isoprene, and CH_2O, as well as the correlation between O_3 and CO, and the O_3-CO regression slopes are reproduced well in the model. The observations show a robust O_3-CO regression in the boundary layer in daytime. We implement a new regression slope decomposition method with four simulated CO tracers, including primary anthropogenic emissions, oxidation of anthropogenic VOCs, oxidation of biogenic isoprene, and transport from model boundaries, to quantify their contributions to the O_3-CO regression slope.

We find that the O_3-CO regression slope in the boundary layer (300 m–2.5 km) is controlled by primary anthropogenic CO emissions and CO production by isoprene oxidation. The contribution by the latter is nearly as large as the former. From 300 m to the surface, the model results indicate that the latter contribution is dominant. Previous studies discussed complicating factors in using the O_3-CO regression slope and the total anthropogenic CO emissions to estimate the net anthropogenic O_3 production amount [e.g., *Chin et al*., 1994; *Parrish et al*., 1998]. Due to the decrease of anthropogenic emissions, our study suggests that biogenic CO needs to be properly accounted for through modeling or measurement means for the eastern United States in the summer when using the O_3-CO regression slope method. The biogenic contribution will continue increasing as anthropogenic emissions decrease. At some point in the future, it can be expected that the biogenic contribution may become the most dominant. Despite the change of the relative importance of anthropogenic and biogenic emissions, the consistent enhancement of O_3 relative to CO observed in the boundary layer, as indicated by the O_3-CO regression slope, provides a useful constraint on model photochemistry and emissions.

Appendix A: Derivation of Equation (1)

CO concentration is the sum of that from primary anthropogenic emissions ($CO_{anthroCO}$), the oxidation of anthropogenic VOCs ($CO_{anthroVOCs}$), the oxidation of biogenic isoprene ($CO_{bioISOP}$), and transport from model lateral and upper boundaries (CO_{BC}):

$$[CO]_{total} = [CO]_{anthroCO} + [CO]_{anthroVOCs} + [CO]_{BC} + [CO]_{bioISOP.} \tag{A1}$$

The slope of O_3 to CO in a least squares regression is thus

$$\text{Least} - \text{squares regression slope} = \frac{Cov(CO_{total}, O_3)}{Var(CO_{total})} \tag{A2}$$

$$= \frac{\overline{\left([CO]_{total} - \overline{[CO]_{total}}\right)\left([O_3] - \overline{[O_3]}\right)}}{Var(CO_{total})} \tag{A3}$$

$$= \frac{\overline{\left([CO]_{anthroCO} + [CO]_{anthroVOCs} + [CO]_{BC} + [CO]_{bioISOP} - \overline{([CO]_{anthroCO} + [CO]_{anthroVOCs} + [CO]_{BC} + [CO]_{bioISOP})}\right)\left([O_3] - \overline{[O_3]}\right)}}{Var(CO_{total})} \tag{A4}$$

$$= \frac{\begin{array}{c}\overline{\left([CO]_{anthroCO} - \overline{[CO]_{anthroCO}}\right)\left([O_3] - \overline{[O_3]}\right)} + \overline{\left([CO]_{anthroVOCs} - \overline{[CO]_{anthroVOCs}}\right)\left([O_3] - \overline{[O_3]}\right)} \\ + \overline{\left([CO]_{BC} - \overline{[CO]_{BC}}\right)\left([O_3] - \overline{[O_3]}\right)} + \overline{\left([CO]_{bioISOP} - \overline{[CO]_{bioISOP}}\right)\left([O_3] - \overline{[O_3]}\right)}\end{array}}{Var(CO_{total})} \tag{A5}$$

$$= \frac{Cov(CO_{anthroCO}, O_3)}{Var(CO_{total})} + \frac{Cov(CO_{anthroVOCs}, O_3)}{Var(CO_{total})} + \frac{Cov(CO_{BC}, O_3)}{Var(CO_{total})} + \frac{Cov(CO_{biolSOP}, O_3)}{Var(CO_{total})}, \quad \text{(A6)}$$

where $\overline{X}$ donates the average value of X.

Acknowledgments
The research was supported by the NASA ACMAP and DISCOVER-AQ programs. The data for this paper are available at the DISCOVER-AQ data archive (http:// www-air.larc.nasa.gov/missions/discover-aq/discover-aq.html).

References

Atkinson, R., and J. Arey (1998), Atmospheric chemistry of biogenic organic compounds, *Acc. Chem. Res.*, *31*(9), 574–583, doi:10.1021/ar970143z.

Bey, I., D. J. Jacob, R. M. Yantosca, J. A. Logan, B. D. Field, A. M. Fiore, Q. Li, H. Y. Liu, L. J. Mickley, and M. G. Schultz (2001), Global modeling of tropospheric chemistry with assimilated meteorology: Model description and evaluation, *J. Geophys. Res.*, *106*(D19), 23,073–23,095, doi:10.1029/2001JD000807.

Brent, L., W. Thorn, M. Gupta, B. Leen, J. Stehr, H. He, H. Arkinson, A. Weinheimer, C. Garland, and S. Pusede (2015), Evaluation of the use of a commercially available cavity ringdown absorption spectrometer for measuring NO_2 in flight, and observations over the Mid-Atlantic States, during DISCOVER-AQ, *J. Atmos. Chem.*, *72*(3–4), 503–521, doi:10.1007/s10874-013-9265-6.

Buhr, M., D. Sueper, M. Trainer, P. Goldan, B. Kuster, F. Fehsenfeld, G. Kok, R. Shillawski, and A. Schanot (1996), Trace gas and aerosol measurements using aircraft data from the North Atlantic Regional Experiment (NARE 1993), *J. Geophys. Res.*, *101*(D22), 29,013–29,027, doi:10.1029/96JD01159.

Cardenas, L., J. Austin, R. Burgess, K. Clemitshaw, S. Dorling, S. Penkett, and R. Harrison (1998), Correlations between CO, NO_y, O_3 and non-methane hydrocarbons and their relationships with meteorology during winter 1993 on the North Norfolk Coast, UK, *Atmos. Environ.*, *32*(19), 3339–3351, doi:10.1016/S1352-2310(97)00445-7.

Chin, M., D. J. Jacob, J. W. Munger, D. D. Parrish, and B. G. Doddridge (1994), Relationship of ozone and carbon monoxide over North America, *J. Geophys. Res.*, *99*(D7), 14,565–14,573, doi:10.1029/94JD00907.

Choi, Y., Y. Wang, T. Zeng, R. V. Martin, T. P. Kurosu, and K. Chance (2005), Evidence of lightning NO_x and convective transport of pollutants in satellite observations over North America, *Geophys. Res. Lett.*, *32*, L02805, doi:10.1029/2004GL021436.

Choi, Y., Y. Wang, Q. Yang, D. Cunnold, T. Zeng, C. Shim, M. Luo, A. Eldering, E. Bucsela, and J. Gleason (2008a), Spring to summer northward migration of high O_3 over the western North Atlantic, *Geophys. Res. Lett.*, *35*, L04818, doi:10.1029/2007GL032276.

Choi, Y., Y. Wang, T. Zeng, D. Cunnold, E. S. Yang, R. Martin, K. Chance, V. Thouret, and E. Edgerton (2008b), Springtime transitions of NO_2, CO, and O_3 over North America: Model evaluation and analysis, *J. Geophys. Res.*, *113*, D20311, doi:10.1029/2007JD009632.

Choi, Y., G. Osterman, A. Eldering, Y. Wang, and E. Edgerton (2010), Understanding the contributions of anthropogenic and biogenic sources to CO enhancements and outflow observed over North America and the western Atlantic Ocean by TES and MOPITT, *Atmos. Environ.*, *44*(16), 2033–2042, doi:10.1016/j.atmosenv.2010.01.029.

Cooper, O., J. Moody, D. Parrish, M. Trainer, T. Ryerson, J. Holloway, G. Hübler, F. Fehsenfeld, and M. Evans (2002a), Trace gas composition of midlatitude cyclones over the western North Atlantic Ocean: A conceptual model, *J. Geophys. Res.*, *107*(D7), 4056, doi:10.1029/2001JD000901.

Cooper, O., J. Moody, D. Parrish, M. Trainer, J. Holloway, G. Hübler, F. Fehsenfeld, and A. Stohl (2002b), Trace gas composition of midlatitude cyclones over the western North Atlantic Ocean: A seasonal comparison of O_3 and CO, *J. Geophys. Res.*, *107*(D7), 4056, doi:10.1029/2001JD000902.

Geng, F., X. Tie, A. Guenther, G. Li, J. Cao, and P. Harley (2011), Effect of isoprene emissions from major forests on ozone formation in the City of Shanghai, China, *Atmos. Chem. Phys.*, *11*(20), 10,449–10,459, doi:10.5194/acp-11-10449-2011.

Gu, D., Y. Wang, C. Smeltzer, and Z. Liu (2013), Reduction in NO_x emission trends over China: Regional and seasonal variations, *Environ. Sci. Technol.*, *47*(22), 12,912–12,919, doi:10.1021/es401727e.

Gu, D., Y. Wang, C. Smeltzer, and K. F. Boersma (2014), Anthropogenic emissions of NO_x over China: Reconciling the difference of inverse modeling results using GOME-2 and OMI measurements, *J. Geophys. Res. Atmos.*, *119*, 7732–7740, doi:10.1002/2014JD021644.

Gu, D., Y. Wang, R. Yin, Y. Zhang, and C. Smeltzer (2016), Inverse modelling of NO_x emissions over eastern China: Uncertainties due to chemical non-linearity, *Atmos. Meas. Tech.*, *9*(10), 5193, doi:10.5194/amt-9-5193-2016.

Guenther, A., C. N. Hewitt, D. Erickson, R. Fall, C. Geron, T. Graedel, P. Harley, L. Klinger, M. Lerdau, and W. McKay (1995), A global model of natural volatile organic compound emissions, *J. Geophys. Res.*, *100*(D5), 8873–8892, doi:10.1029/94JD02950.

Guenther, A. B., X. Jiang, C. L. Heald, T. Sakulyanontvittaya, T. Duhl, L. K. Emmons, and X. Wang (2012), The Model of Emissions of Gases and Aerosols from Nature version 2.1 (MEGAN2. 1): An extended and updated framework for modeling biogenic emissions, *Geosci. Model Dev.*, *5*, 1471–1492, doi:10.5194/gmd-5-1471-2012.

Hassler, B., et al. (2016), Analysis of long-term observations of NO_x and CO in megacities and application to constraining emissions inventories, *Geophys. Res. Lett.*, *43*, 9920–9930, doi:10.1002/2016GL069894.

Honrath, R., R. C. Owen, M. Val Martin, J. Reid, K. Lapina, P. Fialho, M. P. Dziobak, J. Kleissl, and D. Westphal (2004), Regional and hemispheric impacts of anthropogenic and biomass burning emissions on summertime CO and O_3 in the North Atlantic lower free troposphere, *J. Geophys. Res.*, *109*, D24310, doi:10.1029/2004JD005147.

Hudman, R. C., L. T. Murray, D. J. Jacob, D. Millet, S. Turquety, S. Wu, D. Blake, A. Goldstein, J. Holloway, and G. Sachse (2008), Biogenic versus anthropogenic sources of CO in the United States, *Geophys. Res. Lett.*, *35*, L04801, doi:10.1029/2007GL032393.

Huntrieser, H., J. Heland, H. Schlager, C. Forster, A. Stohl, H. Aufmhoff, F. Arnold, H. Scheel, M. Campana, and S. Gilge (2005), Intercontinental air pollution transport from North America to Europe: Experimental evidence from airborne measurements and surface observations, *J. Geophys. Res.*, *110*, D01305, doi:10.1029/2004JD005045.

Jing, P., D. Cunnold, Y. Choi, and Y. Wang (2006), Summertime tropospheric ozone columns from Aura OMI/MLS measurements versus regional model results over the United States, *Geophys. Res. Lett.*, *33*, L17817, doi:10.1029/2006GL026473.

Kesselmeier, J., and M. Staudt (1999), Biogenic volatile organic compounds (VOC): An overview on emission, physiology and ecology, *J. Atmos. Chem.*, *33*, 23–88, doi:10.1023/A:1006127516791.

Koo, J.-H., Y. Wang, T. Kurosu, K. Chance, A. Rozanov, A. Richter, S. Oltmans, A. Thompson, J. Hair, and M. Fenn (2012), Characteristics of tropospheric ozone depletion events in the Arctic spring: Analysis of the ARCTAS, ARCPAC, and ARCIONS measurements and satellite BrO observations, *Atmos. Chem. Phys.*, *12*(20), 9909–9922, doi:10.5194/acp-12-9909-2012.

Lathière, J., D. A. Hauglustaine, A. D. Friend, N. De NobletDucoudré, N. Viovy, and G. A. Folberth (2006), Impact of climate variability and land use changes on global biogenic volatile organic compound emissions, *Atmos. Chem. Phys.*, *6*, 2129–2146, doi:10.5194/acp-6-2129-2006.

Lee, K.-Y., K.-H. Kwak, Y.-H. Ryu, S.-H. Lee, and J.-J. Baik (2014), Impacts of biogenic isoprene emission on ozone air quality in the Seoul metropolitan area, *Atmos. Environ.*, *96*, 209–219, doi:10.1016/j.atmosenv.2014.07.036.

Lelieveld, J., and F. J. Dentener (2000), What controls tropospheric ozone?, *J. Geophys. Res.*, *105*(D3), 3531–3551, doi:10.1029/1999JD901011.

Li, Q., D. J. Jacob, I. Bey, P. I. Palmer, B. N. Duncan, B. D. Field, R. V. Martin, A. M. Fiore, R. M. Yantosca, and D. D. Parrish (2002), Transatlantic transport of pollution and its effects on surface ozone in Europe and North America, *J. Geophys. Res.*, *107*(D13), 4166, doi:10.1029/2001JD001422.

Lindinger, W., A. Hansel, and A. Jordan (1998), Proton-transfer-reaction mass spectrometry (PTR-MS): On-line monitoring of volatile organic compounds at pptv levels, *Chem. Soc. Rev.*, *27*(5), 347–354, doi:10.1039/a827347z.

Liu, Z., Y. Wang, D. Gu, C. Zhao, L. G. Huey, R. Stickel, J. Liao, M. Shao, T. Zhu, and L. Zeng (2010), Evidence of reactive aromatics as a major source of peroxy acetyl nitrate over China, *Environ. Sci. Technol.*, *44*(18), 7017–7022, doi:10.1021/es1007966.

Liu, Z., Y. Wang, M. Vrekoussis, A. Richter, F. Wittrock, J. P. Burrows, M. Shao, C. C. Chang, S. C. Liu, and H. Wang (2012a), Exploring the missing source of glyoxal (CHOCHO) over China, *Geophys. Res. Lett.*, *39*, L10812, doi:10.1029/2012GL051645.

Liu, Z., Y. Wang, D. Gu, C. Zhao, L. Huey, R. Stickel, J. Liao, M. Shao, T. Zhu, and L. Zeng (2012b), Summertime photochemistry during CAREBeijing-2007: RO_x budgets and O_3 formation, *Atmos. Chem. Phys.*, *12*(16), 7737–7752, doi:10.5194/acp-12-7737-2012.

Liu, Z., Y. Wang, F. Costabile, A. Amoroso, C. Zhao, L. G. Huey, R. Stickel, J. Liao, and T. Zhu (2014), Evidence of aerosols as a media for rapid daytime HONO production over China, *Environ. Sci. Technol.*, *48*(24), 14,386–14,391, doi:10.1021/es504163z.

Logan, J. A., M. J. Prather, S. C. Wofsy, and M. B. McElroy (1981), Tropospheric chemistry: A global perspective, *J. Geophys. Res.*, *86*(C8), 7210–7254, doi:10.1029/JC086iC08p07210.

Mao, H., and R. Talbot (2004), O_3 and CO in New England: Temporal variations and relationships, *J. Geophys. Res.*, *109*, D21304, doi:10.1029/2004JD004913.

Pang, X., Y. Mu, Y. Zhang, X. Lee, and J. Yuan (2009), Contribution of isoprene to formaldehyde and ozone formation based on its oxidation products measurement in Beijing, China, *Atmos. Environ.*, *43*(13), 2142–2147, doi:10.1016/j.atmosenv.2009.01.022.

Parrish, D., M. Trainer, J. Holloway, J. Yee, M. Warshawsky, F. Fehsenfeld, G. Forbes, and J. Moody (1998), Relationships between ozone and carbon monoxide at surface sites in the North Atlantic region, *J. Geophys. Res.*, *103*(D11), 13,357–13,376, doi:10.1029/98JD00376.

Parrish, D. D., J. S. Holloway, M. Trainer, P. C. Murphy, F. C. Fehsenfeld, and G. L. Forbes (1993), Export of North American ozone pollution to the North Atlantic Ocean, *Science*, *259*(5100), 1436–1439, doi:10.1126/science.259.5100.1436.

Parrish, D. D., M. Trainer, D. Hereid, E. J. Williams, K. J. Olszyna, R. A. Harley, J. F. Meagher, and F. C. Fehsenfeld (2002), Decadal change in carbon monoxide to nitrogen oxide ratio in US vehicular emissions, *J. Geophys. Res.*, *107*(D12), 4140, doi:10.1029/2001JD000720.

Pierce, T., C. Geron, L. Bender, R. Dennis, G. Tonnesen, and A. Guenther (1998), Influence of increased isoprene emissions on regional ozone modeling, *J. Geophys. Res.*, *103*(D19), 25,611–25,629, doi:10.1029/98JD01804.

Real, E., K. S. Law, H. Schlager, A. Roiger, H. Huntrieser, J. Methven, M. Cain, J. Holloway, J. Neuman, and T. Ryerson (2008), Lagrangian analysis of low altitude anthropogenic plume processing across the North Atlantic, *Atmos. Chem. Phys.*, *8*(24), 7737–7754, doi:10.5194/acp-8-7737-2008.

Sachse, G. W., G. F. Hill, L. O. Wade, and M. G. Perry (1987), Fast-response, high-precision carbon monoxide sensor using a tunable diode laser absorption technique, *J. Geophys. Res.*, *92*(D2), 2071–2081, doi:10.1029/JD092iD02p02071.

Sindelarova, K., C. Granier, I. Bouarar, A. Guenther, S. Tilmes, T. Stavrakou, J. F. Müller, U. Kuhn, P. Stefani, and W. Knorr (2014), Global data set of biogenic VOC emissions calculated by the MEGAN model over the last 30 years, *Atmos. Chem. Phys.*, *14*(17), 9317–9341, doi: 10.5194/acp-14-9317-2014.

Wang, Y., and D. J. Jacob (1998), Anthropogenic forcing on tropospheric ozone and OH since preindustrial times, *J. Geophys. Res.*, *103*, 31,123–31,135, doi:10.1029/1998JD100004.

Wang, Y., and T. Zeng (2004), On tracer correlations in the troposphere: The case of ethane and propane, *J. Geophys. Res.*, *109*, D24306, doi:10.1029/2004JD005023.

Wang, Y., D. J. Jacob, and J. A. Logan (1998), Global simulation of tropospheric O_3-NO_x-hydrocarbon chemistry: 1. Model formulation, *J. Geophys. Res.*, *103*(D9), 10,713–10,725, doi:10.1029/98JD00158.

Wang, Y., Y. Choi, T. Zeng, B. Ridley, N. Blake, D. Blake, and F. Flocke (2006), Late-spring increase of trans-Pacific pollution transport in the upper troposphere, *Geophys. Res. Lett.*, *33*, L01811, doi:10.1029/2005GL024975.

Wang, Y., Y. Choi, T. Zeng, D. Davis, M. Buhr, L. G. Huey, and W. Neff (2007), Assessing the photochemical impact of snow NO_x emissions over Antarctica during ANTCI 2003, *Atmos. Environ.*, *41*(19), 3944–3958, doi:10.1016/j.atmosenv.2007.01.056.

Weibring, P., D. Richter, J. Walega, L. Rippe, and A. Fried (2010), Difference frequency generation spectrometer for simultaneous multispecies detection, *Opt. Express*, *18*(26), 27,670–27,681, doi:10.1364/OE.18.027670.

Yang, Q., Y. Wang, C. Zhao, Z. Liu, W. I. Gustafson Jr., and M. Shao (2011), NO_x emission reduction and its effects on ozone during the 2008 Olympic Games, *Environ. Sci. Technol.*, *45*(15), 6404–6410, doi:10.1021/es200675v.

Zeng, T., Y. Wang, K. Chance, E. V. Browell, B. A. Ridley, and E. L. Atlas (2003), Widespread persistent near-surface ozone depletion at northern high latitudes in spring, *Geophys. Res. Lett.*, *30*(24), 2298, doi:10.1029/2003GL018587.

Zeng, T., Y. Wang, K. Chance, N. Blake, D. Blake, and B. Ridley (2006), Halogen-driven low-altitude O_3 and hydrocarbon losses in spring at northern high latitudes, *J. Geophys. Res.*, *111*, D17313, doi:10.1029/2005JD006706.

Zhang, R., et al. (2017), Enhanced trans-Himalaya pollution transport to the Tibetan Plateau by cut-off low systems, *Atmos. Chem. Phys.*, *17*, 3083–3095, doi:10.5194/acp-17-1-2017.

Zhang, Y., and Y. Wang (2016), Climate-driven ground-level ozone extreme in the fall over the Southeast United States, *Proc. Natl. Acad. Sci.*, *113*, 10025–10030, doi:10.1073/pnas.1602563113.

Zhang, Y., Y. Wang, G. Chen, C. Smeltzer, J. Crawford, J. Olson, J. Szykman, A. J. Weinheimer, D. J. Knapp, and D. D. Montzka (2016), Large vertical gradient of reactive nitrogen oxides in the boundary layer: Modeling analysis of DISCOVER-AQ 2011 observations, *J. Geophys. Res. Atmos. 121*, 1922–1934, doi:10.1002/2015JD024203.

Zhao, C., and Y. Wang (2009), Assimilated inversion of NO_x emissions over East Asia using OMI NO_2 column measurements, *Geophys. Res. Lett.*, *36*, L06805, doi:10.1029/2008GL037123.

Zhao, C., Y. Wang, Y. Choi, and T. Zeng (2009a), Summertime impact of convective transport and lightning NO_x production over North America: Modeling dependence on meteorological simulations, *Atmos. Chem. Phys.*, *9*(13), 4315–4327, doi:10.5194/acp-9-4315-2009.

Zhao, C., Y. Wang, and T. Zeng (2009b), East China plains: A "basin" of ozone pollution, *Environ. Sci. Technol.*, *43*(6), 1911–1915, doi:10.1021/es8027764.

Zhao, C., Y. Wang, Q. Yang, R. Fu, D. Cunnold, and Y. Choi (2010), Impact of East Asian summer monsoon on the air quality over China: View from space, *J. Geophys. Res.*, *115*, D09301, doi:10.1029/2009JD012745.